Current Biology 24, 1845–1853, August 18, 2014 ©2014 Elsevier Ltd All rights reserved http://dx.doi.org/10.1016/j.cub.2014.07.011

Article

# Integrin-Associated Complexes Form Hierarchically with Variable Stoichiometry in Nascent Adhesions

**Alexia I. Bachir,[1,*] Jessica Zareno,[1] Konstadinos Moissoglu,[2] Edward F. Plow,[3] Enrico Gratton,[4] and Alan R. Horwitz[1]**

[1]Department of Cell Biology, University of Virginia, Charlottesville, VA 22908, USA
[2]Center for Cancer Research, National Cancer Institute, National Institutes of Health, Bethesda, MD 20892, USA
[3]Department of Molecular Cardiology, Lerner Research Institute, Cleveland Clinic, Cleveland, OH 44195, USA
[4]Laboratory of Fluorescence Dynamics, Department of Biomedical Engineering, University of California, Irvine, Irvine, CA 92697, USA

## Summary

**Background:** A complex network of putative molecular interactions underlies the architecture and function of cell-matrix adhesions. Most of these interactions are implicated from coimmunoprecipitation studies using expressed components, but few have been demonstrated or characterized functionally in living cells.

**Results:** We introduce fluorescence fluctuation methods to determine, at high spatial and temporal resolution, "when" and "where" molecular complexes form and their stoichiometry in nascent adhesions (NAs). We focus on integrin-associated molecules implicated in integrin activation and in the integrin-actin linkage in NAs and show that these molecules form integrin-containing complexes hierarchically within the adhesion itself. Integrin and kindlin reside in a molecular complex as soon as adhesions are visible; talin, although also present early, associates with the integrin-kindlin complex only after NAs have formed and in response to myosin II activity. Furthermore, talin and vinculin association precedes the formation of the integrin-talin complex. Finally, α-actinin enters NAs periodically and in clusters that transiently associate with integrins. The absolute number and stoichiometry of these molecules varies among the molecules studied and changes as adhesions mature.

**Conclusions:** These observations suggest a working model for NA assembly whereby transient α-actinin-integrin complexes help nucleate NAs within the lamellipodium. Subsequently, integrin complexes containing kindlin, but not talin, emerge. Once NAs have formed, myosin II activity promotes talin association with the integrin-kindlin complex in a stoichiometry consistent with each talin molecule linking two integrin-kindlin complexes.

## Introduction

Cell-matrix adhesion is central to many modes of cell migration, a process involved in pathologies such as cancer, atherosclerosis, and chronic inflammatory diseases [1]. Adhesions are comprised of networks of molecular interactions [2] and generate traction and signals that mediate and regulate migration [3]. Integrin receptors are central components of this network [4]. They bind several different extracellular matrix ligands, organize signaling complexes, and connect to the actin cytoskeleton through interactions with a large number of different molecules that bind to them either directly or indirectly [2, 5]. Despite a plethora of information on the in vitro binding interactions among integrin- and adhesion-associated molecules, "where" and "when" these interactions occur determines adhesion and cellular function and remains largely unknown.

Talin and kindlin bind integrin directly and regulate both its activation and the formation of adhesions [6]. Talin1 knockdown shows diminished activation of $\alpha_{IIb}\beta_3$, $\alpha_v\beta_3$, and $\alpha_5\beta_1$ integrins [7] and impaired adhesion formation [8]. Kindlins, more recently identified as adhesion components [9], are also required for talin-mediated integrin activation [10]. Kindlin3-deficient platelets, for example, fail to activate integrins despite normal talin expression [11]. While the overlapping functions of these two molecules are clear, "when" and "where" talin and kindlin cooperate to activate integrins during adhesion formation is not known. Current models suggest either simultaneous or sequential binding of both molecules to the cytoplasmic tail of the β integrin subunit [12].

A similar conundrum exists for the interactions between integrin and its associated actin-binding adhesion partners. Talin, vinculin, and α-actinin are all thought to be part of a linkage, between integrin and the actin cytoskeleton, that is required for traction and adhesion formation [13, 14]. Both talin and α-actinin bind integrin and actin directly [15, 16]. Vinculin binds talin and activates it; it also binds to actin and α-actinin [17, 18] and, like α-actinin and talin, serves to link integrins to actin filaments and, indirectly, cluster integrins [18, 19]. Thus, even with this small set of molecules, there are many potential interactions that mediate the linkages from integrin to actin. It seems unlikely that all exist simultaneously, but how all of these potential interactions occur and the adhesion types in which they reside is also not known. Further, it is unclear whether these molecules are recruited independently or whether they reside as preformed, preactivated cytoplasmic complexes.

These are only a few of the ~200 molecules thought to associate with adhesions [2]. Their interactions have been inferred largely from immunoprecipitations using purified, endogenous, or overexpressed components. To date, few studies have addressed their existence and function in living cells [14, 20–23]. Recent developments in fluorescence fluctuation methods provide a toolbox for addressing these kinds of molecular interactions [20, 24, 25]. The methods rely on the analysis of molecular intensity fluctuations from fluorescently tagged adhesion molecules and provide measurements of dynamics, concentrations, and aggregation states. When implemented in a dual-color mode, cofluctuations in fluorescence intensity reveal the presence and composition of molecular complexes.

In this study, we introduce fluorescence fluctuation methods to determine at high spatial and temporal resolution the formation and stoichiometry of molecular complexes in the nascent adhesions (NAs) that populate protrusions in

*Correspondence: ab8su@virginia.edu

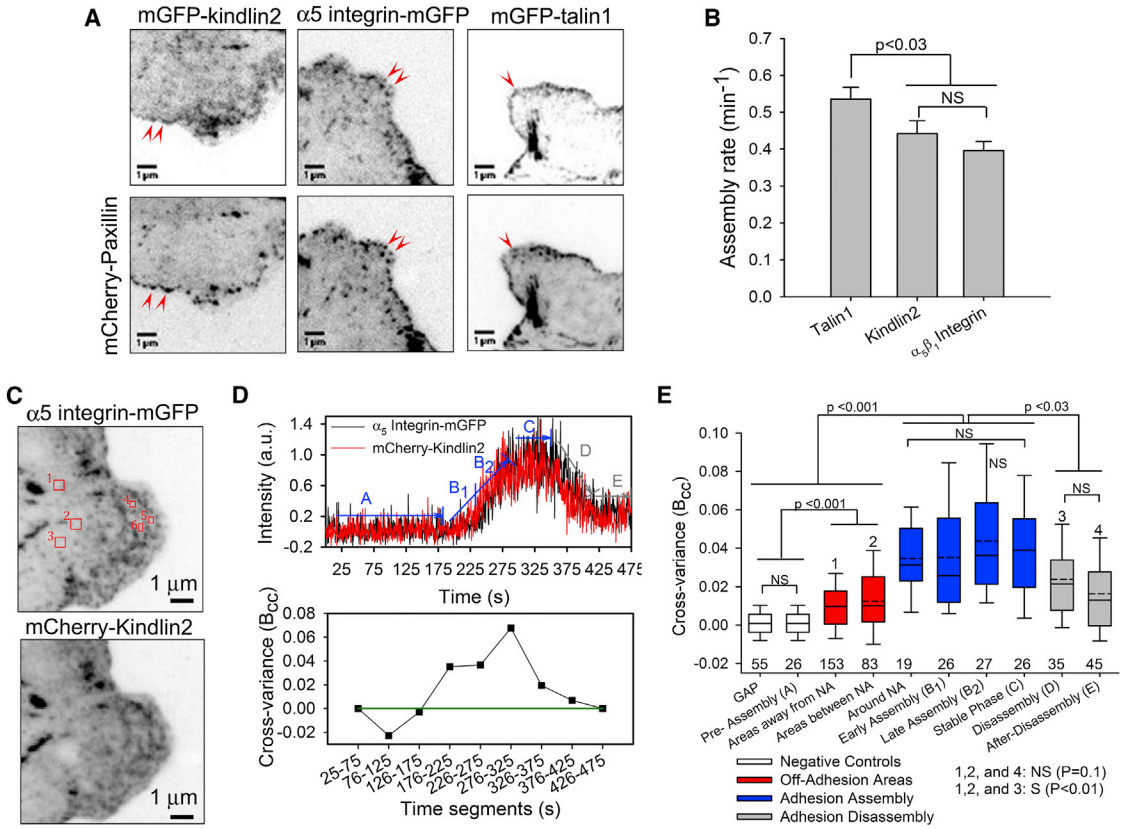


Figure 1. Cross-variance of $\alpha_5\beta_1$ Integrin and Kindlin2 in NAs

(A and B) $\alpha_5$ integrin colocalizes with talin1 and kindlin2 in NAs (arrows; A) with variable assembly rates (B) in CHOK1 cells cotransfected with mCherry-paxillin and the designated GFP-tagged plasmid.

(C) Total internal reflection fluorescence (TIRF) images (average over 50 s) of $\alpha_5$ integrin-mGFP and mCherry-kindlin2 used for cross-variance analysis.

(D) Fluorescence intensity time trace of $\alpha_5$ integrin-mGFP and mCherry-kindlin2 in a selected NA and the corresponding cross-variance or ($B_{cc}$) values calculated from phases of adhesion formation and disassembly (labeled A–E).

(E) Box plot of the ($B_{cc}$) values from pixel regions corresponding to both adhesions and regions without adhesions. ($B_{cc}$) values calculated from areas away (n = 17) and between (n = 19) adhesions were averaged over 5 × 5 and 3 × 3 pixel regions, respectively. For areas between adhesions, ($B_{cc}$) values corresponding to time segments when no adhesions were visible yet were discarded. ($B_{cc}$) values for regions around adhesions were calculated from single square pixel regions surrounding the adhesion. GAP (GAP-mGFP and GAP-mCherry) constitutes a negative control. Images were acquired every 500 ms. Error bars indicate the SEM. See also Figure S1.

migrating CHO cells. We focus on kindlin, talin, vinculin, and α-actinin, integrin-associated molecules implicated in integrin activation or crosslinking to the actin cytoskeleton. We show that whereas these molecules are recruited at the same time to adhesions, their interactions emerge hierarchically within the adhesion itself instead of entering as performed complexes from the neighboring cell membrane or cytoplasm. $\alpha_5\beta_1$ integrin and kindlin2 are detected in a molecular complex at the onset of NA formation; however, talin1 associates with $\alpha_5\beta_1$ integrin and kindlin2 only after NAs have formed and in response to myosin II activity. In contrast, talin1 and vinculin are present in a complex as the NAs assemble. Furthermore, α-actinin enters adhesions in periodic clusters that associate transiently with integrins. We also show that the stoichiometries underlying these interactions vary as adhesions mature. Whereas $\alpha_5\beta_1$ integrin and kindlin2 are present in a 1:1 ratio in NAs, talin is present in a 0.5:1 ratio with integrin. However, as adhesions mature, talin1 increases to a 1:1 ratio with $\alpha_5\beta_1$ integrin and kindlin2. Together, these results point to a hierarchical formation of molecular interactions during NA formation.

## Results

### $\alpha_5\beta_1$ Integrin and Kindlin2 Associate in a Molecular Complex as Adhesions Assemble

To determine whether talin and kindlin reside in NAs, we coexpressed mCherry-paxillin, an early marker of NAs [26], with monomeric GFP (mGFP)-tagged talin1, kindlin2, or the $\alpha_5$ integrin subunit in CHOK1 cells. $\alpha_5\beta_1$ integrin, talin1, and kindlin2 all localize to NAs (Figure 1A, arrowheads) and enter at about the same time, but with differing assembly rates (Figure 1B). Whereas $\alpha_5\beta_1$ integrin and kindlin2 enter with indistinguishable kinetics, talin1 entered slightly faster. These data suggest that the entry of talin is uncoupled from that of either $\alpha_5\beta_1$ integrin or kindlin2 and raise the possibility that the latter two may enter as a preformed complex.

To determine whether the similar assembly rates for $\alpha_5\beta_1$ integrin and kindlin2 in NAs are due to molecular associations that form before or as adhesions assemble, we used cross-variance analysis [24]. This method detects the presence of molecular complexes using covariance analysis of fluorescence fluctuations arising from the dynamic exchange of

molecular complexes in adhesions. Molecules that are unassociated will enter and leave adhesions independently and show no cross-variance or ($B_{cc}$); however, molecules that reside in a common complex will enter and leave together and show a positive cross-variance.

We calculated temporal maps of ($B_{cc}$) using image time series of CHOK1 cells expressing $\alpha_5$ integrin-mGFP and mCherry-kindlin2 (Figure 1C). Figure 1D is a representative plot of the fluorescence intensity of $\alpha_5\beta_1$ integrin and kindlin2 in a NA and the corresponding ($B_{cc}$) values calculated from different stages of adhesion formation. We observed positive ($B_{cc}$) values as the adhesions start to assemble, and they persisted after the adhesions formed. We observed a similar positive ($B_{cc}$) value for the positive controls, mGFP-talin1-mCherry and mCherry-paxillin-mGFP, throughout NA formation (Figure S2 available online). In contrast, the ($B_{cc}$) values measured in pixels before the adhesions were visible and from a negative control consisting of two noninteracting molecules, GAP-mGFP and GAP-mCherry, showed minimal cross-variance (Figure 1E). Furthermore, cells expressing $\alpha_5\beta_1$ integrin and a kindlin2 mutant (Q614A/W615A) that lacks integrin binding activity [27] show neither specific localization to adhesions nor positive cross-variance (Figure S1). These data suggest that $\alpha_5\beta_1$ integrin and kindlin2 reside in a common complex as adhesions form and stabilize (Figure 1E). We also observed lower ($B_{cc}$) values during disassembly and after disassembly, suggesting that some adhesion molecules dissociate from disassembling adhesions independently rather than in complexes.

To determine whether $\alpha_5\beta_1$ integrin and kindlin2 are preassociated before adhesions form, we compared the ($B_{cc}$) values in adhesions with areas outside adhesions, i.e., between NAs (e.g., areas 1–3) and farther away (e.g., areas 4–6) from the adhesion-rich protrusive edge (Figures 1C and 1E). In both of these regions, the ($B_{cc}$) values were calculated from more than 15 areas in each region. Even though the results were statistically above background (negative controls and preassembly pixels in regions where adhesions emerge), they were also statistically different from the ($B_{cc}$) values calculated from the assembly and stability phases, showing that $\alpha_5\beta_1$ integrin and kindlin2 are most likely not associated in a complex at those locations. Taken together, the data suggest that $\alpha_5\beta_1$ integrin and kindlin2 do not interact in the plasma membrane outside adhesions, but rather they assemble into a complex as they enter the adhesion itself.

### Talin Associates with $\alpha_5\beta_1$ Integrin and Kindlin2 after NAs Assemble and in Response to Myosin II Activation

We next determined whether talin1 associates with $\alpha_5\beta_1$ integrin in adhesions by using cross-variance analysis on CHOK1 cells expressing $\alpha_5$ integrin-mGFP and mCherry-talin1. The ($B_{cc}$) values were near control values as the adhesions assembled but then showed positive cross-variance once the NAs formed (Figure 2A). This contrasts kindlin2 and $\alpha_5\beta_1$ integrin, which reside in a complex as NAs assemble. A talin1 mutant (R358A) that does not bind integrins showed weaker localization, more-diffuse expression, and no detectable cross-variance (Figure S1) [28].

Next, we investigated associations between talin1 and kindlin2 using mGFP-talin1 and mCherry-kindlin2. Like talin1 and $\alpha_5\beta_1$ integrin, they did not show statistically significant cross-variance values as NAs assembled but did show positive ($B_{cc}$) values once the NAs assembled (Figure 2B). This reveals that mGFP-talin1 and mCherry-kindlin2 do not reside in a common complex until NAs have assembled, as observed for talin1 and $\alpha_5\beta_1$ integrin. Taken together, these observations show that whereas talin1, kindlin2, and $\alpha_5\beta_1$ integrin all enter NAs as they begin to form, kindlin2 and $\alpha_5\beta_1$ integrin associate in a complex early, during the assembly process, and talin enters the complex after the adhesions have assembled.

Since we observed a delayed association between talin1 and $\alpha_5\beta_1$ integrin in adhesions, we next asked whether it reflects the myosin-dependent maturation into focal complexes and focal adhesions (FAs) [26]. To distinguish between these, we inhibited myosin II activation using Y27632, an inhibitor of ROCK activity and adhesion maturation [29]. When we treated U2OS cells expressing $\alpha_5$ integrin-mGFP and talin-mCherry with 30 $\mu$M Y27632, NAs formed, but they did not mature into elongated adhesions (Figure 2C). mCherry-talin1 localized in these NAs (Figure 2D); however, it did not show detectable ($B_{cc}$) values with $\alpha_5$ integrin-mGFP, even at time periods well beyond those when complexes are detected in control cells (Figure 2E). In contrast, kindlin2 showed positive cross-variance with $\alpha_5\beta_1$ integrin in NAs, even after ROCK inhibition, as it did in untreated controls (Figure 2F). These data suggest that $\alpha_5\beta_1$ integrin-kindlin2 interactions are independent of ROCK-mediated myosin II activation, whereas $\alpha_5\beta_1$ integrin-talin1 interactions require it, demonstrating a possible role for myosin II activity in the formation of a stable talin-integrin complex. These observations agree with studies showing that force coupling mediated through local depletion of PtdIns(4,5)P2 regulates talin but not kindlin recruitment to adhesions [30].

### Talin and Vinculin Reside in a Molecular Complex as Adhesions Assemble and Mature

Since vinculin is implicated in talin activation and incorporation into adhesions [18, 31], we used cross-variance analysis to determine when they associate in NAs. In cells expressing vinculin-mGFP and mCherry-talin1 (Figure 3A), positive cross-variance between talin1 and vinculin appeared at the onset of NA formation (Figures 3A and 3B) and persisted even after the adhesions formed and elongated (Figure 3B). These data suggest that talin1 and vinculin reside in a complex as NAs form and mature. Interestingly, positive ($B_{cc}$) values were predominant at the end, proximal to the protrusion of the elongated adhesions, suggesting a preferential, localized recruitment of the complex (Figure 3C). Furthermore, faster sampling was required to capture the exchange of talin and vinculin as a complex when compared to the sampling time for talin1 and $\alpha_5\beta_1$ integrin, showing that they exchange independently of integrin (Figure S2). This association is not apparent in the cytoplasm via use of ccRICS (Figure S3), but rather emerges in adhesions where force-mediated vinculin activation, required for talin binding [32, 33], is thought to occur [34].

### $\alpha$-Actinin Displays a Distinct Pattern of Entry and Complex Formation in NAs

$\alpha$-actinin binds $\beta_1$ integrin in vitro and is thought to be part of the integrin-actin linkage [15]. To determine "if" and "when" $\alpha$-actinin and integrin associate in a complex, we studied their relative rates of entry in NAs using CHOK1 cells expressing $\alpha_5$ integrin-mGFP and $\alpha$-actinin-mCherry (Figure 4A). $\alpha$-actinin entered NAs at a rate faster than that of $\alpha_5\beta_1$ integrin (Figure 4B). Its intensity increased in periodic spikes (Figure 4A), with an average period of approximately 20 s, suggesting it enters adhesions in discrete clusters. We often also observed small intensity increases for $\alpha_5$ integrin coincident with the $\alpha$-actinin spikes, suggesting that they may be associated. The cross-variance analysis revealed positive ($B_{cc}$) values for

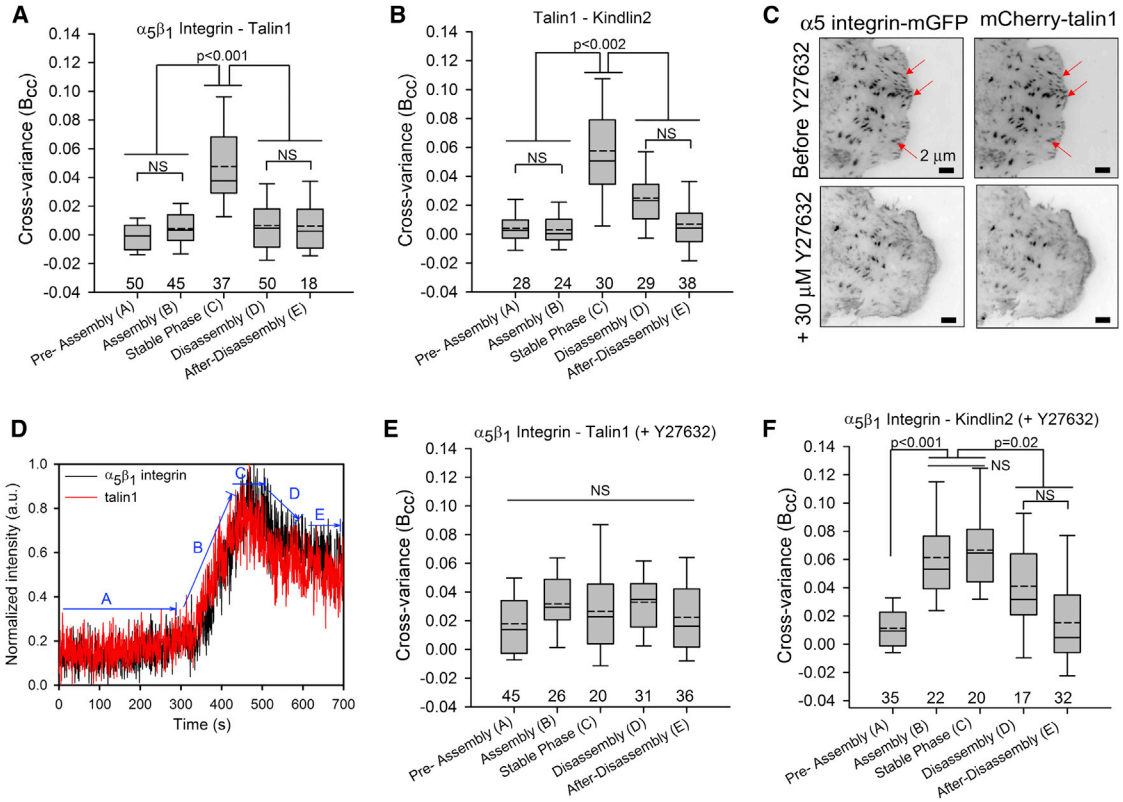


Figure 2. Cross-variance of Talin-$\alpha_5\beta_1$ Integrin, and Talin-Kindlin2 in NAs

(A and B) Box plots of ($B_{cc}$) values calculated for phases of NA formation in CHOK1 cells expressing $\alpha_5\beta_1$ integrin-mGFP and mCherry-talin1 (A) and mGFP-talin1 and mCherry-kindlin2 (B).

(C and D) Intensity images (averaged over 3 min) of U2OS cells expressing $\alpha_5\beta_1$ integrin-GFP and mCherry-talin1 before and 8 min after treatment with Y27632 drug (C). As shown in (D), note that the $\alpha_5\beta_1$ integrin-mGFP- and mCherry-talin1-containing NAs do not mature into larger adhesions similar to those highlighted by arrows in (C).

(E and F) Box plot of ($B_{cc}$) values measured from NAs in cells treated with Y27632 drug show abolished associations between $\alpha_5\beta_1$ integrin-mGFP and mCherry-talin1 (E), but not between $\alpha_5\beta_1$ integrin-mGFP and mCherry-kindlin2 (F). Images were acquired every 500 ms.

See also Figure S1.

$\alpha$-actinin and $\alpha_5\beta_1$ integrin only during the periodic $\alpha$-actinin intensity spikes, showing that, indeed, the molecules transiently associate at discrete, relatively short times during NA assembly (Figure 4C).

This contrasts talin1, which forms molecular complexes with $\alpha_5\beta_1$ integrin only after NAs have formed. We then asked whether the delayed association between integrin and talin1 during NA formation is due to $\alpha$-actinin binding [35]. To do this, we measured the onset of molecular complex formation between integrin and talin1 in CHOK1 cells with $\alpha$-actinin knocked down. Interestingly, talin1 overexpression rescues the inhibition of adhesion and protrusion in the $\alpha$-actinin knockdowns [26] (Figure 4D) and therefore is able to substitute for it during adhesion formation. Furthermore, talin is now present with integrin in molecular complexes as NAs form (Figure 4E). Thus, in the absence of $\alpha$-actinin, talin associates with $\alpha_5\beta_1$ integrin, which is the only integrin present in CHOK1 cells, to rescue the formation and turnover of NAs.

### $\alpha_5\beta_1$ Integrin Displays Differing Stoichiometry Relative to Its Binding Partners

Since integrin actin-binding partners possess multiple binding sites as well as dimerization domains, which could serve to crosslink them to each other as well as to integrins [6, 31, 36], we estimated the number of molecules and stoichiometry of these molecules using fluctuation methods (see the Supplemental Information and Figures S4 and S5). By comparing the NA intensities to the intensity of a known monomer (GAP-mGFP), we estimated that there are ~6.5 ± 1.3 $\alpha_5\beta_1$ integrins in a NA; this is ~2-fold higher than that in pixels adjacent to the NAs (Figure 5A). These $\alpha_5\beta_1$ integrins also reside in adhesions in aggregates with an average of ~6 ± 1 molecules and in off-adhesion regions with an average aggregate of ~2 ± 1 molecules (Figure 5B). Our off-adhesion results are consistent with previous measurements of integrin membrane numbers [25], as well as with fibronectin-integrin binding studies showing that fibronectin trimers are sufficient for binding to the actin cytoskeleton [37].

We next determined the effect of integrin expression level and matrix density on the numbers of integrins in adhesions. In low expressing cells, fewer adhesions formed, and for those that did form, the number of molecules was similar to that seen in off-adhesion regions (Figure 5A). In contrast, the fibronectin density did not affect the number of integrin molecules in adhesions within the 5-fold range that promoted adhesion (Figure 5C). This suggests that the number of integrin molecules in NAs is primarily dictated by intrinsic factors rather than fibronectin density.

We then compared the relative numbers of kindlin2, talin1, and vinculin to $\alpha_5\beta_1$ integrin. Whereas the numbers of kindlin2 and

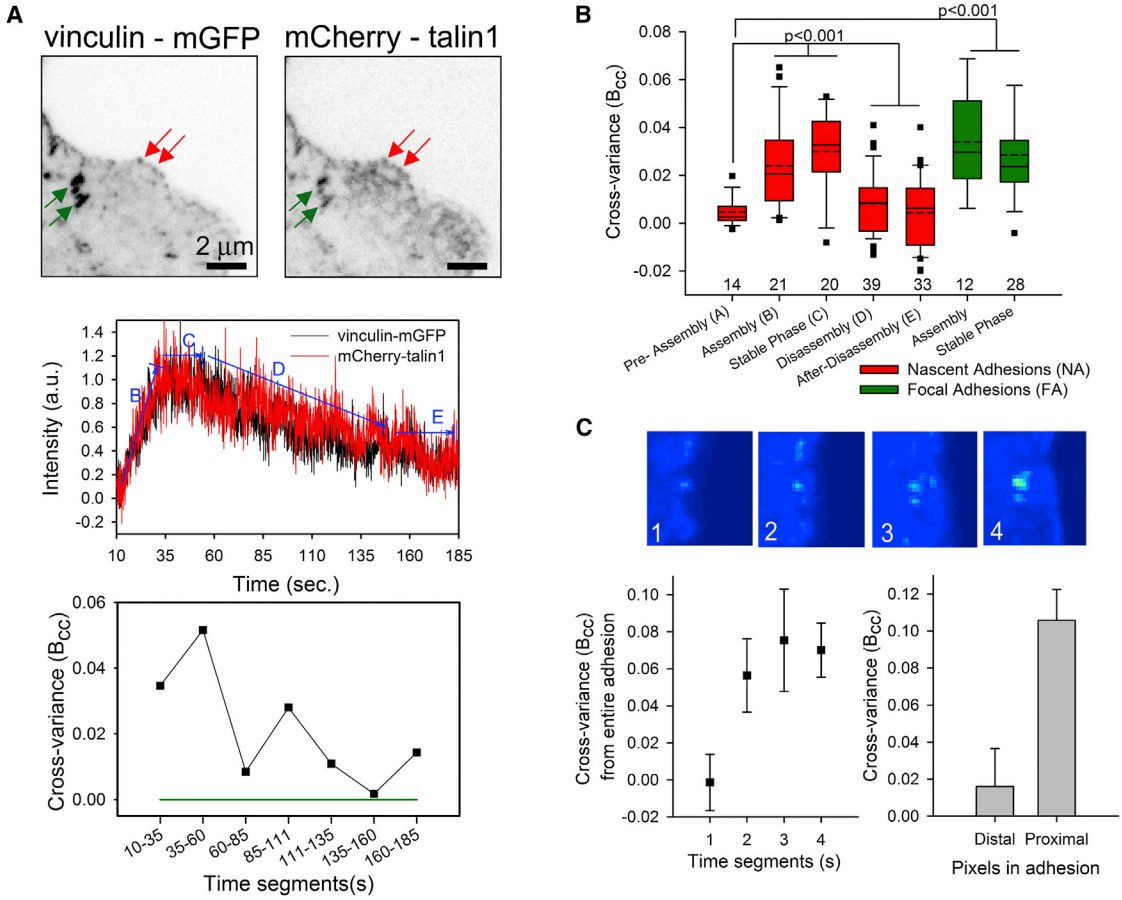


Figure 3. Cross-variance of Talin1 and Vinculin in Adhesions

(A) Vinculin-mGFP and mCherry-talin1 localize to NAs and FAs in CHOK1 cells. Representative fluorescence time traces and ($B_{cc}$) values for vinculin-mGFP and mCherry-talin1 in a NA that disassembles are shown.

(B) Box plot of the ($B_{cc}$) values calculated at different times during NA formation and from adhesions that stabilize into larger FAs, inferring that they reside in a common complex. The ($B_{cc}$) values for the pixels corresponding to individual FAs (n = 5) were averaged over the time segments.

(C) Images from selected time segments in the vinculin time series depict the formation of a NA that matures into a FA by elongating perpendicular to the direction of the protrusion. Different ($B_{cc}$) values at the distal versus proximal regions relative to the protrusion suggest a differential exchange of the molecular complex in different regions of the elongating adhesion.

Error bars indicate the SEM. See also Figures S2 and S3.

integrin were similar (1:1), the number of talin1 molecules was approximately one-half that of $\alpha_5\beta_1$ integrin, values that are also supported by variance analysis of the integrin-talin-kindlin complex. Vinculin displayed ~1.3 times the number of integrin molecules in the NAs; the variability was much greater when compared to kindlin2, talin1, and $\alpha_5\beta_1$ integrin, with more adhesions exhibiting a higher number of molecules (Figure 5D). $\alpha$-actinin numbers in individual NAs was the largest among all molecules. The number of molecules in each $\alpha$-actinin intensity spike contained three to four molecules reaching a plateau of 14 molecules per NA (Figure 5E). Furthermore, for mature elongated FAs, we observed a linear increase in all adhesion molecules as the size of the adhesion increased (Figure 5F). The relative vinculin density was the highest (four times the other molecules), whereas the stoichiometry between kindlin2, talin1, and $\alpha_5\beta_1$ integrin was 1:1, in agreement with previous observations [14].

## Discussion

A complex network of molecular interactions underlies the signaling activities and extracellular matrix (ECM)-actin linkage of cell adhesions [2] and is particularly apparent in an integrated cellular process like migration [5]. Despite the plethora of biochemical information identifying potential interactions among the molecules in cell adhesions, their location, dynamics, stoichiometry, and regulation are largely unknown. To date, the absence methods that capture molecular associations and numbers robustly with high spatial and temporal resolution have challenged their measurement.

In this study, we identify integrin complexes that contain integrin-activating molecules, like kindlin and talin, and actin-linking molecules, like talin, vinculin, and $\alpha$-actinin, during the formation of NAs. We also measure the number of these molecules in the adhesions. We do this by extending and optimizing newly developed fluorescence fluctuation methods, which can produce high-spatial- and high-temporal-resolution maps of protein complexes [20, 24]. We find that all of the molecules studied enter NAs as they first become visible; however, their rate of addition, absolute numbers, and incorporation into molecular complexes in adhesions differs. For example, integrin-kindlin and talin-vinculin are present in complexes as soon as they appear in adhesions, whereas talin-integrin and

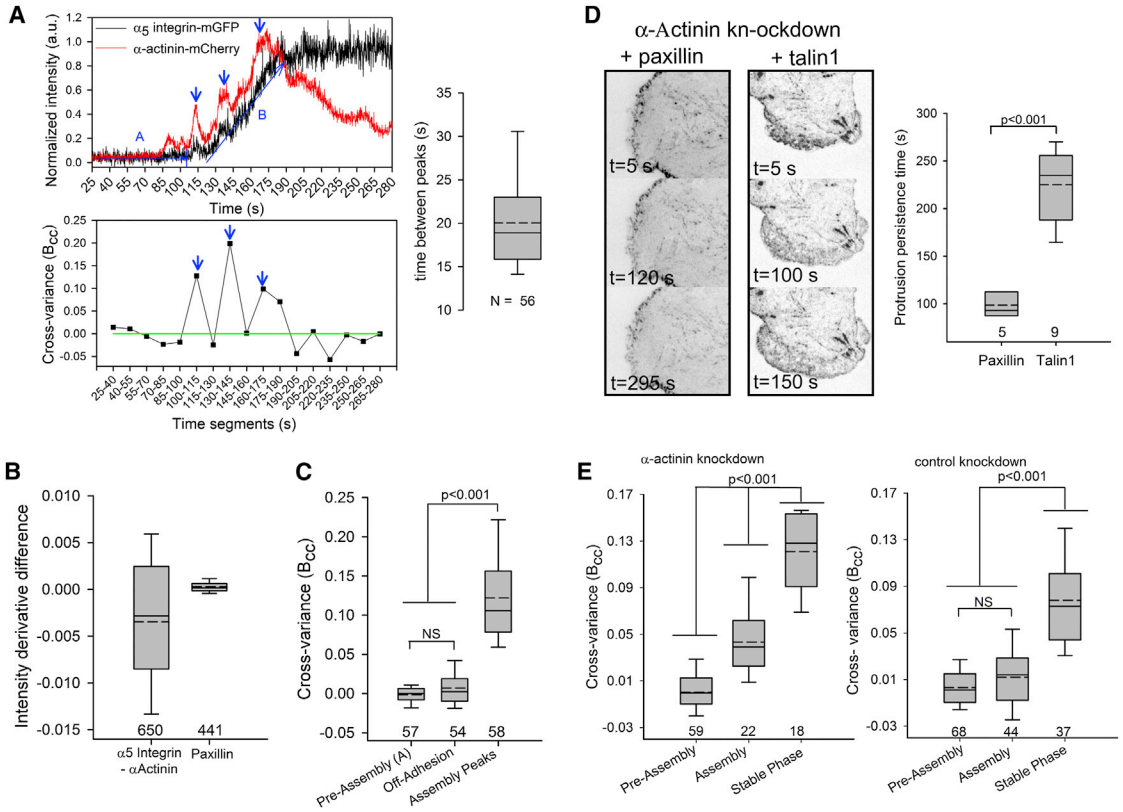


Figure 4. $\alpha_5\beta_1$ Integrin and α-Actinin Assembly and Association in NAs

(A) Intensity time trace of $\alpha_5$ integrin-mGFP and α-actinin-mCherry in a NA in CHOK1 cells. Arrows show α-actinin intensity spikes during assembly and the average duration between the intensity spikes.

(B) The difference in the intensity derivative during assembly for $\alpha_5$ integrin-mGFP and α-actinin-mCherry, in comparison to mCherry-paxillin-GFP, indicates that α-actinin assembles at a faster rate relative to $\alpha_5\beta_1$ integrin.

(C) High positive ($B_{cc}$) values correspond to the α-actinin intensity peaks during NA assembly, whereas no cross-variance is detected in pixels corresponding to regions between adhesions (off adhesions).

(A–C) Twenty-five adhesions were used for quantifications.

(D) α-actinin knockdown in CHOK1 cells expressing talin1-mGFP and mGFP-paxillin. In contrast to paxillin, cells expressing talin1 show persistent protrusive activity.

(E) Effect of α-actinin knockdown on the association of $\alpha_5\beta_1$ integrin and talin1 during NA formation. For cross-variance analysis, images were acquired every 100 ms for mCherry-paxillin-mGFP, 150 ms for integrin-α-actinin, and 500 ms for integrin-talin1.

kindlin-talin reside in common molecular complexes only after the adhesion has formed. In contrast, α-actinin enters at the fastest rate and in spikes that form transient associations with integrin.

The differential molecular associations between integrin and two of its binding partners, kindlin and talin, in adhesions bears on their role in integrin function. Considerable in vitro and in vivo evidence suggests that integrin activation requires the binding of both kindlin and talin [7, 10]. Our cross-variance data suggest that this occurs after NAs have already formed and not in regions adjacent to the adhesions. Therefore, $\alpha_5\beta_1$ integrin is most likely not preactivated before NAs have formed, which is not consonant with observations that integrin is preactivated at the leading edge [38, 39]. This could be due to the different integrin studied ($\alpha_v\beta_3$ versus $\alpha_5\beta_1$) or to the lower resolution, which did not resolve NAs. Our data also do not support a model in which the binding of $\alpha_5\beta_1$ integrin to talin directly nucleates NAs, as they do not appear to reside in a complex until after the NA has formed. Since talin is present in NAs, as soon as they are visible, its interaction with some other molecule(s), like vinculin, RIAM [40, 41], or FAK [42] most likely recruits it to adhesions. Finally, the talin-kindlin-integrin complex, and therefore integrin activation, requires myosin II, presumably through crosslinking and force generation activities [43].

Our observations extend previous studies. Talin-null cells have only small adhesions that adhere weakly and do not mature. Thus, adhesions can form without talin, but they are unable to support or respond to the subsequent force that drives their maturation [8]. This is supported by recent findings that suggest that integrin binding to fibronectin [44] and recruitment to adhesions is independent of talin [22], possibly due to competitive binding with α-actinin [35]. Our data also support suggestions that kindlin and talin associate with integrins sequentially [45, 46], with kindlin associating first and then talin [12]. The initial binding of kindlin might be required to facilitate talin-integrin binding via displacement of integrin inhibitors such as filamin from the β integrin cytoplasmic tail [47] and recruitment of ILK [48] and migfilin [9, 49]. Previous observations also show that NAs can form without myosin II activity, whereas myosin crosslinking and force are required for their subsequent adhesion maturation [26, 50]. Our studies show that the

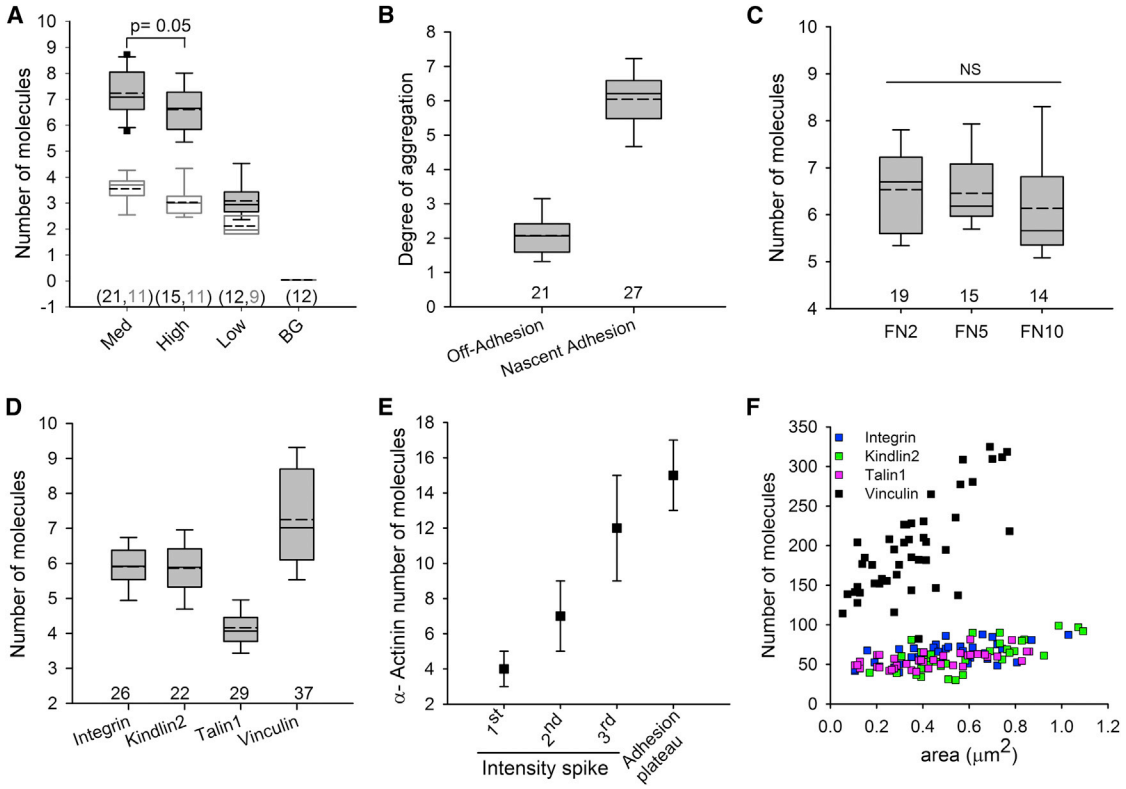


Figure 5. The Number of $\alpha_5\beta_1$ Integrins and Its Partners in Adhesions

(A) Number of molecules of $\alpha_5\beta_1$ integrin as a function of expression level in NAs that stabilize. Expression level is classified based on the average intensity of $\alpha_5\beta_1$ integrin in protruding regions of CHOB2 cells, which lack endogenous $\alpha_5\beta_1$, stably expressing ectopic $\alpha_5$ integrin-mGFP.

(B) Degree of aggregation of $\alpha_5\beta_1$ integrin in NAs.

(C) Number of molecules of $\alpha_5\beta_1$ integrin as a function of variable fibronectin coating concentrations.

(D) Number of molecules of $\alpha_5\beta_1$ integrin, kindlin2, talin1, and vinculin in nascent adhesions.

(E) $\alpha$-actinin numbers in NAs and in the intensity peaks that form during assembly selected from 25 adhesions (see Figure 4). The step size of the $\alpha$-actinin spikes was measured as the difference between the peak intensity of the $n^{th}$ spike and the trough intensity of the $(n-1)^{th}$ peak. For the first intensity peak, we used the preassembly intensity levels to determine the step size.

(F) Number of molecules of $\alpha_5\beta_1$ integrin, kindlin2, talin1, and vinculin in focal adhesions (as a function of size).

Error bars indicate the SEM. See also Figures S4 and S5.

talin-integrin complex is myosin II sensitive, which is consistent with studies showing that integrin, talin, and vinculin are all thought to undergo force induced conformation changes and/or sense force in adhesions [30, 34, 51, 52]. Force in adhesions also stabilizes integrin-fibronectin binding interactions [52].

So, what interactions nucleate adhesions and their subsequent maturation? The number and cluster analyses provide insights. The clustering of integrins is thought to be an early event [53–55]. Since kindlin is monomeric with a single integrin binding site and is present in a 1:1 ratio with integrin in NAs, it is unlikely that it directly mediates the initial clustering of integrins. However, its association with other binding partners, like ILK and migfilin, could indirectly induce clustering [48, 49, 56]. $\alpha$-actinin, another candidate, is a homodimer, binds actin, and is present throughout the lamellipodium in a high stoichiometry with respect to integrin in adhesions. However, if it does nucleate adhesions, it does so only transiently and through large clusters. Once adhesions begin to mature, talin could be a primary link to actin and mediate integrin clustering, since its ratio to integrin is 1:2, suggesting that it crosslinks either through the two integrin binding sites at its N-terminal head and C-terminal tail domains [16] or through its binding to vinculin, which binds to $\alpha$-actinin.

In summary, the integrin binding and actin linkage molecules that we have studied are all present in NAs as soon as they are visible and persist as they mature; however, the molecular interactions and stoichiometry change, reflecting an internal reorganization as the adhesion forms and matures. It is still not clear which molecular interactions drive adhesion formation. Some models propose that integrins are prebound to activating partners at the cell edge and probe the ECM for adhesion sites [38, 39]. Other studies show that adhesion formation is driven by actin polymerization and organization [26]. While kindlin and $\alpha$-actinin remain viable candidates for nucleating adhesion formation through their early association with integrin, the dimeric nature of $\alpha$-actinin and its transient association with $\alpha_5\beta_1$ integrin makes it an attractive potential nucleator. The large $\alpha$-actinin clusters that associate transiently with integrin contain the same number of molecules (three) as those for the off-adhesion integrin clusters, suggesting that $\alpha$-actinin may facilitate an initial binding step of integrin clusters to the actin cytoskeleton, which is then replaced by a longer-lived interaction, and then ultimately by talin [35]. Whatever model emerges, however, it will now be informed by our observation that an important class of integrin interactions occurs transiently and hierarchically within the adhesion.

## Experimental Procedures

### NA Analysis

The NAs were manually selected in protruding regions, and the corresponding pixel locations were inputted in MATLAB 7.7.0 (MathWorks). The fluorescence intensity time traces for individual adhesions were measured by spatial averaging of a 3 × 3 pixel region centered at the adhesion pixel location for each image in the time series. Background intensity was corrected for by subtracting from an image series an average intensity value corresponding to background regions away from the cell. Fluorescence bleaching was estimated using the intensity decay of FAs over the time course of image series acquisition. It was then accounted for by adding to each image in the image series the percent of intensity lost at that given time point. Adhesion assembly rates were estimated from 30–40 adhesions in six to eight cells as in [26]. In the measurements of the number of molecules, the intensities of individual adhesions were integrated over a 3 × 3 pixel region for NAs and over the entire pixel location of larger FAs. For α-actinin number measurements in NAs, we subtracted an average intensity corresponding to lamellipodial regions where no adhesions are visible. To yield the total number of molecules, we normalized the intensity values of the adhesions by the molecular fluorescence of mGFP (for more information, see the Supplemental Information and Supplemental Experimental Procedures).

### Fluorescence Variance and Cross-variance Analysis

We used fluorescence variance analysis, also known as number and brightness (N&B), to determine the aggregation states and molecular interactions (cross-N&B) in adhesions [24]. Using SimFCS software (Laboratory of Fluorescence Dynamics, University of California, Irvine), we calculated the apparent brightness, (B), and cross-brightness, ($B_{cc}$), parameters from single- or dual-channel image time series. The apparent brightness, $B(x_i,y_j)$, parameter for a given pixel location, $(x_i,y_j)$, in a single-channel image time series is defined as

$$B(x_i,y_j)=\frac{1}{S}\cdot\frac{\sigma^2_{i,j}-\sigma^2_0}{\langle I(x_i,y_j)\rangle_t\text{-offset}}=\varepsilon+1, \qquad \text{(Equation 1)}$$

where $\langle I(x_i,y_j)\rangle_t$ and $\sigma^2_{i,j}$ are the pixel average intensity and variance over time ($t$), respectively, and $\varepsilon$ is the intrinsic molecular brightness, which reflects the total number of emitting molecules in a complex and can vary depending on the image acquisition settings that affect fluorescence excitation and detection.

The offset parameter and readout noise, $\sigma^2_0$, were determined from the distribution of the digital counts of a background region in the image time series. The $S$ factor was set to a value that yields a background brightness value of 1(B/S = 1). Contributions from slow fluctuations due to photobleaching and mechanical drift effects were corrected for using a moving-average filter (~20–25 s). The aggregation state of adhesion molecules was determined by calibration of the measured apparent brightness parameter relative to that measured from the membrane targeting sequence of mGFP tagged GAP43 [20].

$$\text{Degree of Aggregation}=\frac{B_{Adh}-1}{B_{GAP}-1} \qquad \text{(Equation 2)}$$

For detection of molecular interactions in adhesions, we calculate the cross-variance, ($B_{cc}$), parameter at a given pixel location, $(x_i,y_j)$, as:

$$B_{cc}(x_i,y_j)=\frac{\sigma(x_i,y_j)^2_{cc}}{\sqrt{\langle I_1(x_i,y_j)\rangle_t\langle I_2(x_i,y_j)\rangle_t}} \qquad \text{(Equation 3)}$$

where $\langle I_1(x_i,y_j)\rangle_t$ and $\langle I_2(x_i,y_j)\rangle_t$ are the fluorescence average intensity for channels 1 and 2. $\sigma(x_i,y_j)^2_{cc}$ is the fluorescence intensity cross-variance between channels 1 and 2 for time, t, and is defined as

$$\sigma(x_i,y_j)^2_{cc}=\frac{1}{t}\cdot\sum_t\left(I_1(x_i,y_j,t)-\langle I_1(x_i,y_j)\rangle_t\right)\cdot\left(I_2(x_i,y_j,t)-\langle I_2(x_i,y_j)\rangle_t\right) \qquad \text{(Equation 4)}$$

where $I_1(x_i,y_j,t)$ and $I_2(x_i,y_j,t)$ are the fluorescence pixel intensity at time, t, for channels 1 and 2, respectively.

If molecules represented by fluorescence intensity in two channels (wavelengths), channels 1 and 2, are noninteracting, their fluorescence fluctuations will be independent and the cross-variance will be centered around zero. In contrast, interacting species will produce positive ($B_{cc}$) values. As the negative control, GAP-mGFP and GAP-mCherry, which localize independently to the cell membrane, are not known to interact and therefore do not display positive cross-variance values [20]. As positive controls, we used mCherry-paxillin-mGFP and mCherry-talin1-mGFP, adhesion markers that are tagged with two fluorescent probes and therefore produce correlated movement and positive cross-variance.

## Supplemental Information

Supplemental Information includes Supplemental Experimental Procedures and five figures and can be found with this article online at http://dx.doi.org/10.1016/j.cub.2014.07.011.

## Acknowledgments

We thank D. Critchley for helpful comments and discussions. This research was supported by NIH grants R01 GM023244 and the Cell Migration Consortium (U54 GM064346) for A.R.H. and by NIH grants NIH P41-GM103540 and NIH P50-GM076516 for E.G.

Received: March 24, 2014
Revised: June 3, 2014
Accepted: July 4, 2014
Published: July 31, 2014

## References

1. Friedl, P., and Gilmour, D. (2009). Collective cell migration in morphogenesis, regeneration and cancer. Nat. Rev. Mol. Cell Biol. *10*, 445–457.
2. Zaidel-Bar, R., Itzkovitz, S., Ma'ayan, A., Iyengar, R., and Geiger, B. (2007). Functional atlas of the integrin adhesome. Nat. Cell Biol. *9*, 858–867.
3. Parsons, J.T., Horwitz, A.R., and Schwartz, M.A. (2010). Cell adhesion: integrating cytoskeletal dynamics and cellular tension. Nat. Rev. Mol. Cell Biol. *11*, 633–643.
4. Hynes, R.O. (2002). Integrins: bidirectional, allosteric signaling machines. Cell *110*, 673–687.
5. Vicente-Manzanares, M., Choi, C.K., and Horwitz, A.R. (2009). Integrins in cell migration—the actin connection. J. Cell Sci. *122*, 199–206.
6. Calderwood, D.A., Campbell, I.D., and Critchley, D.R. (2013). Talins and kindlins: partners in integrin-mediated adhesion. Nat. Rev. Mol. Cell Biol. *14*, 503–517.
7. Tadokoro, S., Shattil, S.J., Eto, K., Tai, V., Liddington, R.C., de Pereda, J.M., Ginsberg, M.H., and Calderwood, D.A. (2003). Talin binding to integrin beta tails: a final common step in integrin activation. Science *302*, 103–106.
8. Zhang, X., Jiang, G., Cai, Y., Monkley, S.J., Critchley, D.R., and Sheetz, M.P. (2008). Talin depletion reveals independence of initial cell spreading from integrin activation and traction. Nat. Cell Biol. *10*, 1062–1068.
9. Tu, Y., Wu, S., Shi, X., Chen, K., and Wu, C. (2003). Migfilin and Mig-2 link focal adhesions to filamin and the actin cytoskeleton and function in cell shape modulation. Cell *113*, 37–47.
10. Ma, Y.Q., Qin, J., Wu, C., and Plow, E.F. (2008). Kindlin-2 (Mig-2): a co-activator of beta3 integrins. J. Cell Biol. *181*, 439–446.
11. Moser, M., Nieswandt, B., Ussar, S., Pozgajova, M., and Fässler, R. (2008). Kindlin-3 is essential for integrin activation and platelet aggregation. Nat. Med. *14*, 325–330.
12. Moser, M., Legate, K.R., Zent, R., and Fässler, R. (2009). The tail of integrins, talin, and kindlins. Science *324*, 895–899.
13. Calderwood, D.A., Shattil, S.J., and Ginsberg, M.H. (2000). Integrins and actin filaments: reciprocal regulation of cell adhesion and signaling. J. Biol. Chem. *275*, 22607–22610.
14. Kanchanawong, P., Shtengel, G., Pasapera, A.M., Ramko, E.B., Davidson, M.W., Hess, H.F., and Waterman, C.M. (2010). Nanoscale architecture of integrin-based cell adhesions. Nature *468*, 580–584.
15. Otey, C.A., Pavalko, F.M., and Burridge, K. (1990). An interaction between alpha-actinin and the beta 1 integrin subunit in vitro. J. Cell Biol. *111*, 721–729.
16. Critchley, D.R. (2009). Biochemical and structural properties of the integrin-associated cytoskeletal protein talin. Annu. Rev. Biophys. *38*, 235–254.
17. Bois, P.R., Borgon, R.A., Vonrhein, C., and Izard, T. (2005). Structural dynamics of alpha-actinin-vinculin interactions. Mol. Cell. Biol. *25*, 6112–6122.

18. Humphries, J.D., Wang, P., Streuli, C., Geiger, B., Humphries, M.J., and Ballestrem, C. (2007). Vinculin controls focal adhesion formation by direct interactions with talin and actin. J. Cell Biol. *179*, 1043–1057.
19. Shen, K., Tolbert, C.E., Guilluy, C., Swaminathan, V.S., Berginski, M.E., Burridge, K., Superfine, R., and Campbell, S.L. (2011). The vinculin C-terminal hairpin mediates F-actin bundle formation, focal adhesion, and cell mechanical properties. J. Biol. Chem. *286*, 45103–45115.
20. Choi, C.K., Zareno, J., Digman, M.A., Gratton, E., and Horwitz, A.R. (2011). Cross-correlated fluctuation analysis reveals phosphorylation-regulated paxillin-FAK complexes in nascent adhesions. Biophys. J. *100*, 583–592.
21. Patla, I., Volberg, T., Elad, N., Hirschfeld-Warneken, V., Grashoff, C., Fässler, R., Spatz, J.P., Geiger, B., and Medalia, O. (2010). Dissecting the molecular architecture of integrin adhesion sites by cryo-electron tomography. Nat. Cell Biol. *12*, 909–915.
22. Rossier, O., Octeau, V., Sibarita, J.B., Leduc, C., Tessier, B., Nair, D., Gatterdam, V., Destaing, O., Albigès-Rizo, C., Tampé, R., et al. (2012). Integrins β1 and β3 exhibit distinct dynamic nanoscale organizations inside focal adhesions. Nat. Cell Biol. *14*, 1057–1067.
23. Zamir, E., Geiger, B., and Kam, Z. (2008). Quantitative multicolor compositional imaging resolves molecular domains in cell-matrix adhesions. PLoS ONE *3*, e1901.
24. Digman, M.A., Wiseman, P.W., Choi, C., Horwitz, A.R., and Gratton, E. (2009). Stoichiometry of molecular complexes at adhesions in living cells. Proc. Natl. Acad. Sci. USA *106*, 2170–2175.
25. Wiseman, P.W., Brown, C.M., Webb, D.J., Hebert, B., Johnson, N.L., Squier, J.A., Ellisman, M.H., and Horwitz, A.F. (2004). Spatial mapping of integrin interactions and dynamics during cell migration by image correlation microscopy. J. Cell Sci. *117*, 5521–5534.
26. Choi, C.K., Vicente-Manzanares, M., Zareno, J., Whitmore, L.A., Mogilner, A., and Horwitz, A.R. (2008). Actin and alpha-actinin orchestrate the assembly and maturation of nascent adhesions in a myosin II motor-independent manner. Nat. Cell Biol. *10*, 1039–1050.
27. Shi, X., Ma, Y.Q., Tu, Y., Chen, K., Wu, S., Fukuda, K., Qin, J., Plow, E.F., and Wu, C. (2007). The MIG-2/integrin interaction strengthens cell-matrix adhesion and modulates cell motility. J. Biol. Chem. *282*, 20455–20466.
28. García-Alvarez, B., de Pereda, J.M., Calderwood, D.A., Ulmer, T.S., Critchley, D., Campbell, I.D., Ginsberg, M.H., and Liddington, R.C. (2003). Structural determinants of integrin recognition by talin. Mol. Cell *11*, 49–58.
29. Narumiya, S., Ishizaki, T., and Uehata, M. (2000). Use and properties of ROCK-specific inhibitor Y-27632. Methods Enzymol. *325*, 273–284.
30. Legate, K.R., Takahashi, S., Bonakdar, N., Fabry, B., Boettiger, D., Zent, R., and Fässler, R. (2011). Integrin adhesion and force coupling are independently regulated by localized PtdIns(4,5)2 synthesis. EMBO J. *30*, 4539–4553.
31. Carisey, A., and Ballestrem, C. (2011). Vinculin, an adapter protein in control of cell adhesion signalling. Eur. J. Cell Biol. *90*, 157–163.
32. Cohen, D.M., Kutscher, B., Chen, H., Murphy, D.B., and Craig, S.W. (2006). A conformational switch in vinculin drives formation and dynamics of a talin-vinculin complex at focal adhesions. J. Biol. Chem. *281*, 16006–16015.
33. Chen, H., Choudhury, D.M., and Craig, S.W. (2006). Coincidence of actin filaments and talin is required to activate vinculin. J. Biol. Chem. *281*, 40389–40398.
34. Carisey, A., Tsang, R., Greiner, A.M., Nijenhuis, N., Heath, N., Nazgiewicz, A., Kemkemer, R., Derby, B., Spatz, J., and Ballestrem, C. (2013). Vinculin regulates the recruitment and release of core focal adhesion proteins in a force-dependent manner. Curr. Biol. *23*, 271–281.
35. Roca-Cusachs, P., del Rio, A., Puklin-Faucher, E., Gauthier, N.C., Biais, N., and Sheetz, M.P. (2013). Integrin-dependent force transmission to the extracellular matrix by α-actinin triggers adhesion maturation. Proc. Natl. Acad. Sci. USA *110*, E1361–E1370.
36. Otey, C.A., and Carpen, O. (2004). Alpha-actinin revisited: a fresh look at an old player. Cell Motil. Cytoskeleton *58*, 104–111.
37. Coussen, F., Choquet, D., Sheetz, M.P., and Erickson, H.P. (2002). Trimers of the fibronectin cell adhesion domain localize to actin filament bundles and undergo rearward translocation. J. Cell Sci. *115*, 2581–2590.
38. Kiosses, W.B., Shattil, S.J., Pampori, N., and Schwartz, M.A. (2001). Rac recruits high-affinity integrin alphavbeta3 to lamellipodia in endothelial cell migration. Nat. Cell Biol. *3*, 316–320.
39. Galbraith, C.G., Yamada, K.M., and Galbraith, J.A. (2007). Polymerizing actin fibers position integrins primed to probe for adhesion sites. Science *315*, 992–995.
40. Lee, H.S., Anekal, P., Lim, C.J., Liu, C.C., and Ginsberg, M.H. (2013). Two modes of integrin activation form a binary molecular switch in adhesion maturation. Mol. Biol. Cell *24*, 1354–1362.
41. Goult, B.T., Zacharchenko, T., Bate, N., Tsang, R., Hey, F., Gingras, A.R., Elliott, P.R., Roberts, G.C., Ballestrem, C., Critchley, D.R., and Barsukov, I.L. (2013). RIAM and vinculin binding to talin are mutually exclusive and regulate adhesion assembly and turnover. J. Biol. Chem. *288*, 8238–8249.
42. Lawson, C., Lim, S.T., Uryu, S., Chen, X.L., Calderwood, D.A., and Schlaepfer, D.D. (2012). FAK promotes recruitment of talin to nascent adhesions to control cell motility. J. Cell Biol. *196*, 223–232.
43. Vicente-Manzanares, M., Ma, X., Adelstein, R.S., and Horwitz, A.R. (2009). Non-muscle myosin II takes centre stage in cell adhesion and migration. Nat. Rev. Mol. Cell Biol. *10*, 778–790.
44. Roca-Cusachs, P., Gauthier, N.C., Del Rio, A., and Sheetz, M.P. (2009). Clustering of alpha(5)beta(1) integrins determines adhesion strength whereas alpha(v)beta(3) and talin enable mechanotransduction. Proc. Natl. Acad. Sci. USA *106*, 16245–16250.
45. Bledzka, K., Liu, J., Xu, Z., Perera, H.D., Yadav, S.P., Bialkowska, K., Qin, J., Ma, Y.Q., and Plow, E.F. (2012). Spatial coordination of kindlin-2 with talin head domain in interaction with integrin β cytoplasmic tails. J. Biol. Chem. *287*, 24585–24594.
46. Kim, C., Ye, F., and Ginsberg, M.H. (2011). Regulation of integrin activation. Annu. Rev. Cell Dev. Biol. *27*, 321–345.
47. Kiema, T., Lad, Y., Jiang, P., Oxley, C.L., Baldassarre, M., Wegener, K.L., Campbell, I.D., Ylänne, J., and Calderwood, D.A. (2006). The molecular basis of filamin binding to integrins and competition with talin. Mol. Cell *21*, 337–347.
48. Mackinnon, A.C., Qadota, H., Norman, K.R., Moerman, D.G., and Williams, B.D. (2002). C. elegans PAT-4/ILK functions as an adaptor protein within integrin adhesion complexes. Curr. Biol. *12*, 787–797.
49. Das, M., Ithychanda, S.S., Qin, J., and Plow, E.F. (2011). Migfilin and filamin as regulators of integrin activation in endothelial cells and neutrophils. PLoS ONE *6*, e26355.
50. Riveline, D., Zamir, E., Balaban, N.Q., Schwarz, U.S., Ishizaki, T., Narumiya, S., Kam, Z., Geiger, B., and Bershadsky, A.D. (2001). Focal contacts as mechanosensors: externally applied local mechanical force induces growth of focal contacts by an mDia1-dependent and ROCK-independent mechanism. J. Cell Biol. *153*, 1175–1186.
51. Grashoff, C., Hoffman, B.D., Brenner, M.D., Zhou, R., Parsons, M., Yang, M.T., McLean, M.A., Sligar, S.G., Chen, C.S., Ha, T., and Schwartz, M.A. (2010). Measuring mechanical tension across vinculin reveals regulation of focal adhesion dynamics. Nature *466*, 263–266.
52. Kong, F., García, A.J., Mould, A.P., Humphries, M.J., and Zhu, C. (2009). Demonstration of catch bonds between an integrin and its ligand. J. Cell Biol. *185*, 1275–1284.
53. Miyamoto, S., Akiyama, S.K., and Yamada, K.M. (1995). Synergistic roles for receptor occupancy and aggregation in integrin transmembrane function. Science *267*, 883–885.
54. Sastry, S.K., and Burridge, K. (2000). Focal adhesions: a nexus for intracellular signaling and cytoskeletal dynamics. Exp. Cell Res. *261*, 25–36.
55. Bunch, T.A. (2010). Integrin alphaIIbbeta3 activation in Chinese hamster ovary cells and platelets increases clustering rather than affinity. J. Biol. Chem. *285*, 1841–1849.
56. Ye, F., Petrich, B.G., Anekal, P., Lefort, C.T., Kasirer-Friede, A., Shattil, S.J., Ruppert, R., Moser, M., Fässler, R., and Ginsberg, M.H. (2013). The mechanism of kindlin-mediated activation of integrin αIIbβ3. Curr. Biol. *23*, 2288–2295.